SPH method applied to high speed cutting modelling

J. Limido[a,*], C. Espinosa[a], M. Salaün[a], J.L. Lacome[b]

[a]DGM, ENSICA, 1 Place Emile Blouin, 31056 Toulouse Cedex 5, France
[b]LSTC, rue du Lanoux, 31330 Grenade sur Garonne, France

Abstract

The purpose of this study is to introduce a new approach of high speed cutting numerical modelling. A Lagrangian smoothed particle hydrodynamics (SPH)-based model is carried out using the Ls-Dyna software. SPH is a meshless method, thus large material distortions that occur in the cutting problem are easily managed and SPH contact control permits a ‘‘natural’’ workpiece/chip separation. The developed approach is compared to machining dedicated code results and experimental data. The SPH cutting model has proved is ability to account for continuous to shear localized chip formation and also correctly estimates the cutting forces, as illustrated in some orthogonal cutting examples. Thus, comparable results to machining dedicated codes are obtained without introducing any adjusting numerical parameters (friction coefficient, fracture control parameter).

Keywords: Smoothed particle hydrodynamics method; Orthogonal cutting; High speed machining

1. Introduction

Machining is the most used process in industrial components production. Aeronautical manufacturers use machining to generate parts submitted to fatigue loads. For a few years, this process has evolved to high speed machining (HSM) because it makes it possible to improve productivity. Fatigue life of machined parts is linked to the surface integrity and so to the machining process. Thus, it is necessary to choose the machining parameters in order to optimize the production quality and the productivity. Creating a predictive cutting model is the first step to achieve this goal. The development of accurate and reliable machining process models has received considerable attention from both academic researchers and industry practitioners in recent years. Traditionally, the techniques used in industry are based on past experience, extensive experimentation, and trial-and-error. Such an approach is time consuming, expensive, and does not lead to a rigorous general scientific knowledge. For years, considerable effort has therefore been devoted to the development of computational models of high-speed machining. Machining modelling is becoming an increasingly important tool in gaining understanding and improving machining processes. Most of the machining numerical models are developed and based on finite element methods (FEM). In a first time dedicated codes have been created but nowadays researches are oriented on creating commercial code-based models.

Here, we present a new approach of the metal cutting modelling by using a smoothed particle hydrodynamics (SPH) Lagrangian method in the frame of the Ls-Dyna FE hydrodynamic code [1,20]. SPH is a meshfree method that originated in 1977 for astrophysics applications. Over the past three decades, the method is being improving and extending to continuum mechanics scales. During the 15 more recent years the method has been proved to be stable in a mathematical point of view [2] and solid stress and strains tensors can now be computed through behaviour laws ranging from pure fluids to brittle solids.

The paper is organized as follows. Prior researches in modelling cutting process are first presented in Section 2. Cutting mechanism and cutting problem specificity are exposed. Then, analytical and FEM models are briefly reviewed to underline the modelling difficulties of the

*Corresponding author. Tel.: +33 561618596; fax: +33 0561618595.
E-mail address: jlimido@ensica.fr (J. Limido).

cutting problem. AdvantEdge [3], a machining dedicated commercial code based on Lagrangian FEM, is briefly presented and analysed. In Section 3, our SPH cutting model is introduced. The SPH method is shortly outlined. Then, the model is precisely described and the constitutive model is analysed. In Section 4, the interests of SPH modelling in cutting problem resolution are discussed by comparisons to existing FEM. Finally, SPH cutting model applications are outlined in Section 5. Two cutting cases that are known to produce, respectively, continuous and shear localized chips are studied with our SPH model and compared to experimental and numerical FEM (AdvantEdge) data.

2. Prior research in modelling cutting process

2.1. Key aspects

The physical phenomena involved in industrial cutting cases are fully 3D and very complex. Thus, most of the prior researches were carried out within the orthogonal cutting framework in order to permit a 2D study. It is still today an interesting study framework because it can be the base of industrial cases studies. Orthogonal cutting conditions are reached when the cutting edge is rectilinear, perpendicular to the chip flow in each point, and perpendicular to the tool feed. In these conditions, the cutting parameters are summarized by cutting speed (Vc) and feed (*f*) (see Fig. 1). In experiments, orthogonal cutting can be obtained by turning a thin walled tube, and setting the cutting edge perpendicular to the tube axis. When the chip thickness remains small in front of its width, the orthogonal cutting can be considered as a two-dimensional (2D) problem. Indeed, edge effects excluded, all the phenomena which take place in the perpendiculars planes of the cutting edge are identical. Thus, the problem can be considered as a 2D plane strain problem.

Comprehension of the chip formation mechanisms is still partial but important information was identified. In orthogonal cutting conditions and in stationary regime, the tool/workpiece interaction and the chip generation process can be represented in a simple way. Three principal shearing zones appear: the primary zone (shearing causing the chip formation), the secondary zone (shearing due to tool/chip friction), and tertiary zone (shearing due to tool/generated surface friction) (see Fig. 1). The tool advance generates pressure on the chip and shear appears between the point of tool and the free surface of the workpiece (primary shear zone). High plastic strain (about 10) and high strain rate (about 10^4–$10^5\,s^{-1}$) are identified in the shear zones. So, an important heat production is generated by plastic strain and friction. Temperature at tool/chip interface can reach about 1000 °C in Titanium alloys machining.

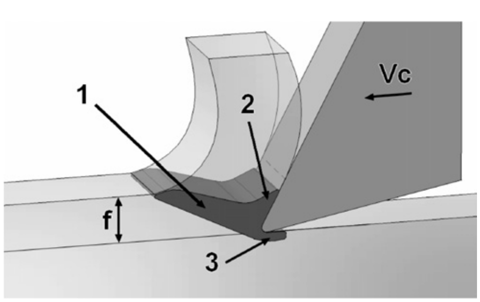

Fig. 1. Shear zones definition.

The metal cutting study has a long history and a large amount of literature is available on this subject. A quick overview is presented here. In 1876, Tresca assumed the plastic deformation as the basic mechanism in the chip formation. This assumption underwent a significant progress in the 1930s in the works of Ernst and Merchant [4]. The Merchant's shear plane model is still considered as very useful, particularly for some approximate solutions. Late Oxley [5] developed a model to predict cutting forces and average temperatures and stresses in the primary and secondary deformation zones. The theory is based on the shear angle determination. Analyzing the stress distributions along the shear plane and the tool–chip interface, the shear angle is selected in order that the resultant forces transmitted by the shear plane and tool–chip interface are in equilibrium. They applied this theory to low carbon steel orthogonal cutting and obtained cutting forces and chip thickness with relatively good results. More recently, Moufki et al. [6] presented an oblique cutting model for viscoplastic materials. This model takes into account thermomechanical properties and inertia effects to describe the material flow in the primary shear zone. The friction law implemented is temperature dependant. They applied the proposed model to oblique cutting analysis of steel and compared results with experiments. The model is shown to lead to predictions of the chip flow angle and cutting forces which are in agreement with the experimental trends. These analytical models are very interesting because they allow a good comprehension of the physical phenomena which intervene during a cutting process and they give good prediction of cutting forces. Nevertheless, none of these models is able to give information about the machined surface, neither in term of roughness, nor in term of residual stresses. Thus, it is a major interest of computational models to give information on the machined surface.

Recent advances in software and hardware technology have made possible to run FEM simulations with 100,000–300,000 or more elements in a reasonable amount of time. Thus, it is nowadays possible to implement FEM-based cutting models; however some important difficulties must be overcome in order to create predictive models.

2.2. Issues and existing numerical models

The first aspect of modelling difficulties is the material behaviour knowledge under the machining conditions. These extreme loading conditions do not allow traditional material characterization like traction test. Thus, it is quite challenging to implement a representative constitutive model of the solicitation that takes into account so high strain, strain rate and temperature. In analytical and numerical cutting models, Johnson and Cook [7] or modified Johnson–Cook [8] constitutive models are generally used because they are relatively simple (5 parameters) and numerically robust. But, any constitutive model needs characterization data to determine its constitutive parameters. These data must be representative of the studied material response under machining loading conditions. In this aim, experimental data are generally obtained at high strain rates and large strains using the split Hopkinson pressure bar method. This test permits to reach strain rates up to 10^3–$10^4\,s^{-1}$ and temperatures up to 600 °C [9].

The choice of a friction model representing the physical phenomena that occur during cutting is also a significant part of the machining modelling problem resolution. Indeed, the friction model influences largely the cutting forces calculated [10]. The Coulomb model is used in most cases in cutting models. It is a very simple model which cannot represent all the friction complexity in machining. The Coulomb friction parameter is often used in order to readjust the cutting forces obtained by FEM compared to the experimental results [10,11].

The third aspect of the modelling difficulties is the correct representation of material separation in front of the tool tip. Typical approaches for numerical modelling of metal cutting are Lagrangian and Eulerian, and arbitrary Lagrangian–Eulerian (ALE) techniques.

Lagrangian approach has been largely applied to metal cutting using FEM [3]. It can be used to simulate from initial to steady state of cutting process. But in order to extend the cutting time until steady state, a long workpiece is needed in geometry modelling, which increases the calculation time. With a Lagrangian formulation, two basically different models are used for the chip separation, a geometrical model and a physical model. The geometrical one is based on the separation of a pre-defined crack path at a certain limit of stresses. In the physical model, the chip formation occurs through the plastic deformation of the elements. Excessive element distortions are avoided by frequently updating the finite element mesh. The physical model seems to be more suitable to simulate the chip formation. Indeed, the geometrical model is unable to predict machined surface integrity because the machined surface is pre-defined. But the Lagrangian approach is not limited to the traditional FEM formulation. Various approaches such as extended finite element method and particle finite element method are currently studied by Guétaria et al. [12] and Oliver et al. [13] in the cutting modelling framework.

Eulerian approach is suitable to analyse the steady state of cutting process, not including the transition from initial to steady-state cutting process, varying cutting thickness in milling operation or serrated chip in high-speed-cutting. Indeed, Eulerian approach is unable to simulate free surface conditions. Cutting process analysis with Eulerian approach requires less calculation time because the workpiece model consists of fewer elements. But experimental work is often necessary in order to determine the chip geometry and shear angle, which is an unavoidable part of geometry modelling.

To handle large deformations and to avoid too much element distortion another approach is mixed arbitrary Lagrangian–Eulerian formulation [3]. This technique combines the advantages of both the Lagrangian and the Eulerian method. Free surfaces are described in a Lagrangian sense and internal nodes can be disconnected from the material displacements to retain a regularly shaped element, like in an Eulerian method. Many cutting models using these different approaches were developed in the last few years but a model is often taken as reference, AdvantEdge [3].

AdvantEdge is an explicit dynamic, thermo-mechanically coupled finite element modelling package specialized for metal cutting including adaptive remeshing capabilities. The chip formation approach is the physical model: no damage or failure criteria are defined assuming that the chip formation is due to plastic flow. Simulations demonstrate the ability of the model to predict continuous and shear localized chip morphologies [3]. This model gives good results in many cases in particular with regard to the cutting forces. Nevertheless, Irander [14] showed that the continuous/shear-localized chip transition is not always well predicted. Moreover, the friction coefficient is used in order to adjust the cutting forces compared to experimental results. The model is thus not fully predictive. Bil et al. [11] compared various computational cutting models (including AdvantEdge) to experimental data. They found that, although individual parameters may match with experimental results, all models failed to achieve a satisfactory correlation with all measured process parameters (see Fig. 2). They suggest that it is due to the chip separation model.

So, in this paper, a new chip separation model is presented using the SPH method implemented in Ls-Dyna.

3. SPH cutting model

3.1. Basic principles of the SPH method [1]

The main advantage of the SPH method is to bypass the requirement for a numerical grid to calculate spatial

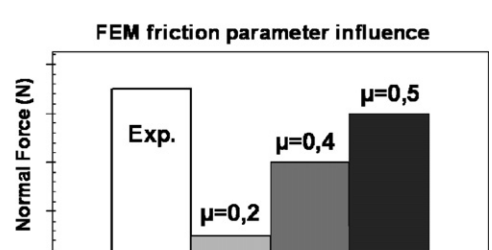

Fig. 2. Effect of friction factor on the thrust force results obtained by AdvantEdge [11].

derivatives. Material properties and state variables are approximated at a discrete set of disordered points, called SPH particles. This avoids severe problems associated with mesh tangling and distortion which usually occur in Lagrangian analyses involving large deformation and/or strain rates and extreme loading events.

Grid-based methods such as Lagrange and Euler FE assume connectivity between nodes to construct spatial derivatives. SPH uses a kernel approximation which is based on randomly distributed interpolation points with no assumptions about which points are neighbours to calculate spatial derivatives. To illustrate this, consider a continuum represented by a set of interacting particles, as shown in Fig. 3. Each particle i interacts with all other particles j that are within a given distance (usually assumed to be 2 h) from it. The distance h is called the smoothing length. The interaction is weighted by the function W which is called the smoothing (or kernel) function. This function has a compact support and is expressed below. Using this principle, the value of a continuous function, or its derivative, can be estimated at any particle i based on known values at the surrounding particles j using the following kernel estimates:

$$\langle f(\mathbf{x})\rangle \approx \int_{\Omega} f(\mathbf{x}')W(\mathbf{x}-\mathbf{x}',h)\,\mathrm{d}\mathbf{x}', \tag{1}$$

$$\langle \nabla\cdot f(\mathbf{x})\rangle \approx \int_{\Omega} [\nabla\cdot f(\mathbf{x}')]W(\mathbf{x}-\mathbf{x}',h)\,\mathrm{d}\mathbf{x}', \tag{2}$$

where f is a function of the 3D position vector $\mathbf{x}$ and $\mathrm{d}\mathbf{x}$ is a volume. To express W, let us introduce an auxiliary function, say θ. The most commonly function used by the SPH community is the cubic B-spline which has some good properties of regularity

$$W(\mathbf{x}-\mathbf{x}',h) = \frac{1}{h^D}\theta\left(\frac{\|\mathbf{x}-\mathbf{x}'\|}{h}\right) \tag{3}$$

with

$$\theta(y) = C \times \begin{cases} 1-\frac{3}{2}y^2+\frac{3}{4}y^3 & \text{for } y \leqslant 1, \\ \frac{1}{4}(2-y)^3 & \text{for } 1 < y \leqslant 2, \\ 0 & \text{for } y > 2, \end{cases} \tag{4}$$

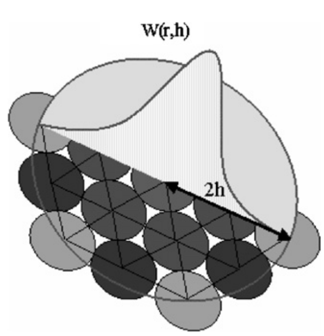

Fig. 3. Neighbouring particle geometry.

where C is a constant of normalization that depends on the space dimension D (see Fig. 3).

Then, the smoothing function W satisfies the following conditions:

Normalization condition:

$$\int_{\Omega} W(\mathbf{x}-\mathbf{x}',h)\,\mathrm{d}\mathbf{x}' = 1. \tag{5}$$

Delta function property:

$$\lim_{h\to 0} W(\mathbf{x}-\mathbf{x}',h) = \delta(\mathbf{x}-\mathbf{x}'), \tag{6}$$

where δ is the Dirac function.

Compact support condition:

$$W(\mathbf{x}-\mathbf{x}',h) = 0 \text{ when } |\mathbf{x}-\mathbf{x}'| > h. \tag{7}$$

3.1.1. Particle approximation of function

After several steps of derivation and by converting the continuous volume integrals to sums over discrete interpolation points, the equations can be expressed into several forms, with commonly used symmetric formulations for the gradient. Ls-Dyna formulation can be expressed as follows:

$$\langle f(x_i)\rangle = \sum_j \frac{m_j}{\rho_j} f(x_j)W(x_i-x_j,h), \tag{8}$$

where m_j is the mass of the particle j and ρ_j is the density of the particle j.

The approximation for the spatial derivative of a function is obtained by applying the derivation operator on the smoothing length.

$$\langle \nabla\cdot f(x_i)\rangle = \sum_j \frac{m_j}{\rho_j} f(x_j)\nabla\cdot W(x_i-x_j,h). \tag{9}$$

The equations of conservation governing the evolution of mechanical variables can be expressed as follows:

Conservation of mass:

$$\frac{\mathrm{d}\rho^i}{\mathrm{d}t} = \rho^i \sum_{j=1}^{N} \frac{m^j}{\rho^j}(v^j_\beta - v^i_\beta)\frac{\partial W^{ij}}{\partial x^i_\beta}. \tag{10}$$

Conservation of momentum:

$$\frac{\mathrm{d}v^i_\alpha}{\mathrm{d}t} = \sum_{j=1}^{N} m^j\left(\frac{\sigma^i_{\alpha\beta}}{\rho^{i2}} - \frac{\sigma^j_{\alpha\beta}}{\rho^{j2}}\right)\frac{\partial W^{ij}}{\partial x^i_\beta}. \tag{11}$$

Conservation of energy:

$$\frac{\mathrm{d}E^i}{\mathrm{d}t} = -\frac{\sigma^i_{\alpha\beta}}{\rho^{i2}}\sum_{j=1}^{N} m^j(v^j_\alpha - v^i_\alpha)\frac{\partial W^{ij}}{\partial x^i_\beta}, \tag{12}$$

where $W^{ij} = W(x^i - x^j, h)$.

3.1.2. Calculation cycle

The basic steps of SPH method used in Ls-Dyna are presented in Fig. 4. The calculation cycle is similar to that for a classical FE computation except for the steps where a

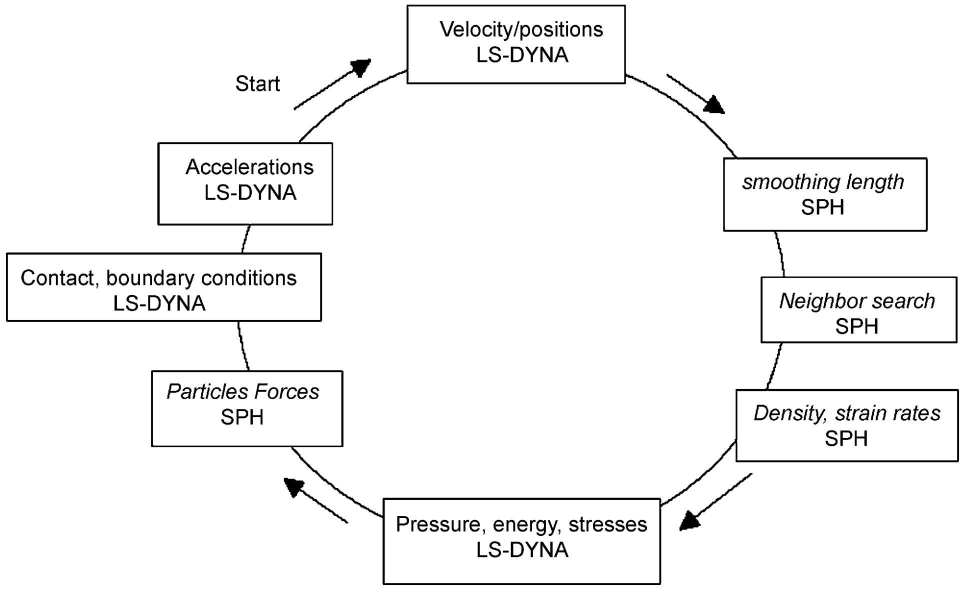

Fig. 4. Computational cycle for SPH methodology in Ls-Dyna.

kernel approximation is used. Kernel approximations are used to compute forces from spatial derivatives of stresses and spatial derivatives of velocity are required to compute strain rates. In addition SPH requires a sort of the particles in order to locate current neighbouring particles ("Neighbours search").

3.2. *Model description*

The numerical cutting model presented here is developed using the SPH method previously described.

3.2.1. *Assumptions*

Several assumptions were made in order to reduce the model size and the computation time, allowing the development of a useful method.

The model is implemented in the orthogonal cutting framework, thus in 2D. The workpiece is reduced to a surface of approximately 7 mm^2. A full 3D model using the SPH method has been developed, but the results, we present here, are obtained with the 2D SPH model.

The tool is supposed to be not deformable and its velocity is imposed. During the process, the computation time is reduced by using a tool velocity ten times higher than the real velocity. This assumption is usually used in simulation of stamping processes [3]. It is valid as long as the accelerated mass is low and as the material behaviour is slightly influenced by the strain rate. These two conditions will be used in Section 5.

3.2.2. *Boundary conditions*

Single point constraints are applied on the back and lower face in order to maintain the part during machining simulation as shown in Fig. 5. It was checked that the stress state in the workpiece is only slightly disturbed by the proximity of the boundary conditions compared to the force introduction.

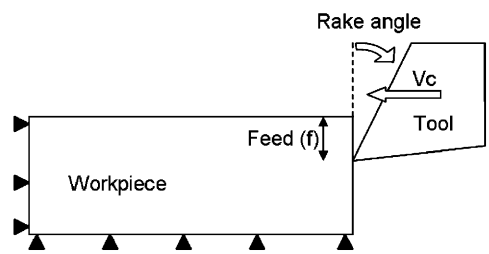

Fig. 5. Boundary conditions.

3.2.3. *SPH density*

Interparticular distance was fixed in order to represent the adiabatic shear band phenomena which the typical dimension is about 20 μm. Then, the whole model is composed of approximately 160,000 particles.

3.2.4. *Material constitutive model*

The flow stress or instantaneous yield strength at which work material starts to plastically deform or flow is mostly influenced by temperature, strain and strain rate. Accurate and reliable flow stress models are considered as highly necessary to represent work material constitutive behaviour under high speed cutting conditions. Semi-empirical constitutive models are widely used. The constitutive model proposed by Johnson and Cook [7] is often used for ductile materials in cases where strain rate vary over a large range and where adiabatic temperature increase due to plastic heating cause material softening. The yield stress ($\bar{\sigma}_y$) depends on the equivalent plastic strain ($\bar{\varepsilon}$), the equivalent plastic strain rate ($\dot{\bar{\varepsilon}}$) and the temperature (T), it is expressed as follows:

$$\bar{\sigma}_y = [A + B(\bar{\varepsilon})^n]\left[1 + C\ln\left(\frac{\dot{\bar{\varepsilon}}}{\dot{\bar{\varepsilon}}_0}\right)\right]\left[1 - \left(\frac{T - T_{room}}{T_{melt} - T_{room}}\right)^m\right]. \quad (13)$$

The parameter A is the initial yield strength of the material at room temperature and a strain rate of 1/s. The strain rate is normalized with a reference strain rate. In general, the Johnson–Cook constitutive model constants A, B, C, n and m are fitted to the data obtained by split Hopkinson pressure bar tests at strain rates up to $10^3\,s^{-1}$ and at temperatures up to 600 °C [9].

All Johnson–Cook parameters used in our model result from the literature.

4. SPH cutting model capabilities compared to classical FEM approach

An overview of the main specificities of the SPH cutting model approach compared to classical Lagrangian FE models is summarized in Table 1. The first column inventories the principal difficulties induced by the use of Lagrangian finite elements for cutting modelling. The solutions classically suggested within the framework of FE are gathered in the second column. The last column shows how the SPH method deals with these aspects. SPH method applied to machining modelling involves several advantages.

First, high strains are easily handled. The particles move relatively to each other in a disordered way during the deformation. This can be considered as a particles rearranging without topological restriction, thus no remeshing is needed.

Another advantage induced by SPH method is the ‘‘natural’’ chip/workpiece separation. The relative movement of the particles creates the opening. The new free surfaces are given by the particles positions. The reader can notice that no specific treatment is done on the ‘‘boundary’’ particles. The opening resistance is taken into account by the interaction of the workpiece particles in the influence sphere. Thus, the workpiece matter ‘‘flows naturally’’ around the tool tip.

In the same way, the SPH method presents an original aspect concerning contact handling. Indeed, the tool particles are velocity imposed and have a mass and strength quite higher than that of the workpiece. As a matter of fact, when a workpiece particle ‘‘sees’’ in its particles neighbours tool particles, then workpiece particle circumvents the tool. Thus, friction is modelled as particles interactions and friction parameter (like Coulomb parameter) does not have to be defined. SPH friction modelling must be studied in-depth (it is a work in progress) but it offers a very interesting alternative to traditional definitions.

The last aspect of the SPH method presented in this part relates to the computational time. It is known to require much CPU time. Nevertheless, Lagrangian methods using adaptive remeshing and ALE methods are also very costly. Moreover, SPH method progress and Batra and Zhang [15] recent work make it possible to think that the implementation of 3D SPH models (oblique cutting applications) will allow computational time equal and even lower than FE models.

Table 1
SPH and classical approach comparison

	Lagrangian FE models	SPH cutting model
Large deformation process	Adaptative remeshing algorithm	SPH meshless nature
New free surfaces creation	Continuous remeshing and fracture model	Particles separation
Contact	Friction Coulomb approach	Particles interactions
Heat generation	Fully thermomechanical coupling	Adiabatic

5. SPH cutting model results compared to a reference FEM

Two applications are presented in the following: these are two cutting cases that are known to produce, respectively, continuous and shear localized chip. They are studied and compared to experimental and numerical FEM (AdvantEdge) data. Comparisons are carried out on the chip morphology, stress distribution and the specific cutting forces.

5.1. Continuous chip: Al6061–T6

The first application concerns Aluminium alloy Al6061–T6. The process parameters are collected in Table 2. The material model parameters result from Lesuer, Leblanc and Kay work [16]. These parameters were

Table 2
Process parameters

Speed (m/s)	Rake angle (deg)	Feed (μm)	Edge radius (μm)
10	5	250	25

Table 3
Material model parameters

A	B	n	C	m
324 MPa	114 MPa	0.42	0.002	1.34

obtained by using split Hopkinson pressure bar method and are gathered in Table 3.

SPH model was carried out without modification of these parameters. All the AdvantEdge and experimental results presented in this part are based on the Marusich work [17].

5.1.1. Chip morphology

Ls-Dyna SPH and AdvantEdge chip morphology results are presented in Figs. 6 and 7. Al6061–T6 is known to produce continuous chip in the speed and feed range studied [17]. SPH and AdvantEdge models results are in agreement with these experimental observations.

The AdvantEdge model overestimates the chip thickness and the Ls-Dyna SPH model underestimates the chip thickness.

As expected, the deformation is largely confined to the primary shear zone and to a boundary layer adjacent to the tool. Fig. 7b shows the stresses map during the continuous chip formation. Primary and secondary shear zone described in Fig. 1 can be easily identified.

5.1.2. Cutting forces

Normal and tangential components of the cutting forces are compared. All simulations were performed with a 25 μm edge radius in order to minimize the introduction of an additional length scale. The Ls-Dyna and AdvantEdge cutting forces are compared in Fig. 8.

Ls-Dyna predicted cutting forces agree within 10% and 30% of the measured values for, respectively, tangential and normal components. These differences can be explained by difference in chip separation criteria, friction model and SPH tool increased velocity assumption. It is important to recall that the SPH model does not have numerical parameter making it possible to control friction. Thus the predicted cutting forces were not adjusted. On the other hand, the AdvantEdge model used a Coulomb parameter fixed to 0.2 without any precision on the method to obtain this value.

5.2. Shear localized chip: AISI4340

The second application concerns AISI4340 high strength steel. The process parameters are collected in Table 4. The material model parameters result from Mabrouki et al.

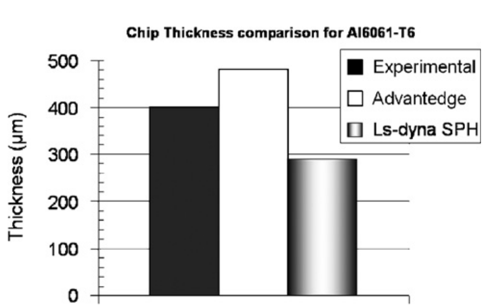

Fig. 6. Al6061–T6 Chip thickness AdvantEdge/Ls-Dyna comparisons.

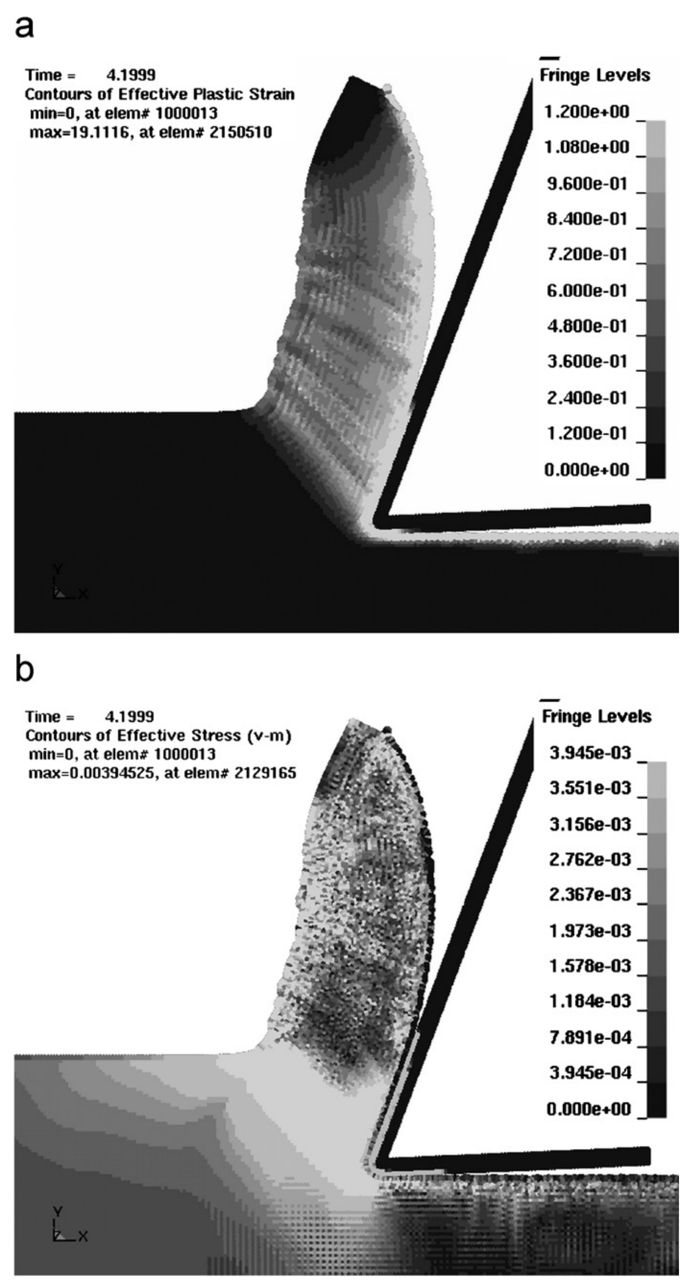

Fig. 7. Al6061–T6 SPH model results: (a) plastic strain, and (b) Von Mises stresses.

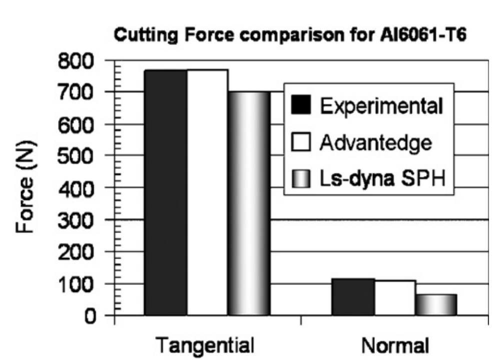

Fig. 8. Al6061–T6 predicted cutting forces comparisons AdvantEdge/Ls-Dyna.

work [18]. These parameters were obtained by using split Hopkinson pressure bar method and are gathered in Table 5.

SPH model was carried out without modification of these parameters. Case 1 and Case 2 AdvantEdge and experimental results presented in this part are based on Ref. [18].

5.2.1. Chip morphology

In the speed and feed range studied, AISI4340 produces shear localized chips (see Fig. 9). Shear localized chips are characterized by oscillatory profiles. They are the result of adiabatic shear band formation in the primary shear zone of the workpiece material. This phenomenon is very well observed and described in Davies and Burns [19].

The local plastic shear instability arise from a competition of the tendency of the material to harden as it deforms, and the opposing tendency of the material to soften if local heating due to plastic dissipation is large enough [19]. These tests make it possible to visualize the influence of the feed on the appearance and the localization of the adiabatic shear bands. The increase in feed induces a more important localization of shear and thus a contracting of the shear band and an increase in the teeth size (Fig. 10).

Table 4
Process parameters

Case	Speed (m/s)	Rake angle (deg)	Feed (μm)	Edge radius (μm)
1	2	−5	250	25
2	2	−5	400	25

Table 5
Material model parameters

A	*B*	*n*	*C*	*m*
910 MPa	586 MPa	0.26	0.014	1.03

Ls-Dyna SPH chip formation results are presented in Figs. 11a, 12 and 13a and the AdvantEdge results are collected in Figs. 11b and 13b. SPH and AdvantEdge models results are in agreement with the experimental observations (see Fig. 9).

The SPH method correctly models all the steps of the cyclic adiabatic shear band formation:

- The tool tip imposes pressure to the cold material ahead of it, and stresses grow in the primary shear band (Fig. 12a).
- The loads reach the cold yield stress of the material and shear begins in the primary shear band (Fig. 12b).
- The great majority of the plastic work is dissipated as heat and the material starts to heat up locally in primary shear zone (Fig. 12c).

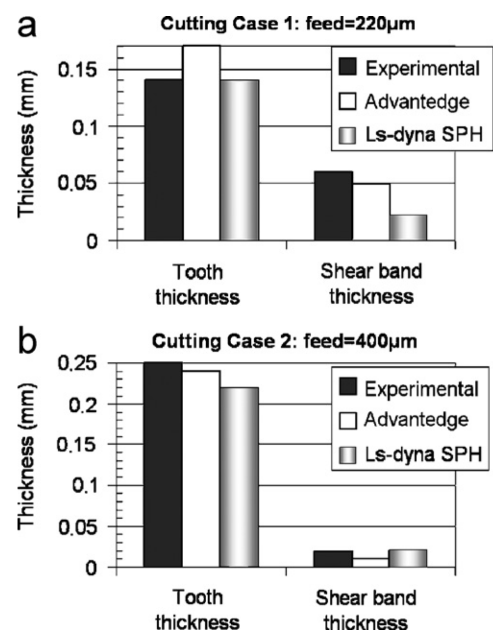

Fig. 10. AISI4340 Chip morphology comparisons: (a) Case 1 and (b) Case 2.

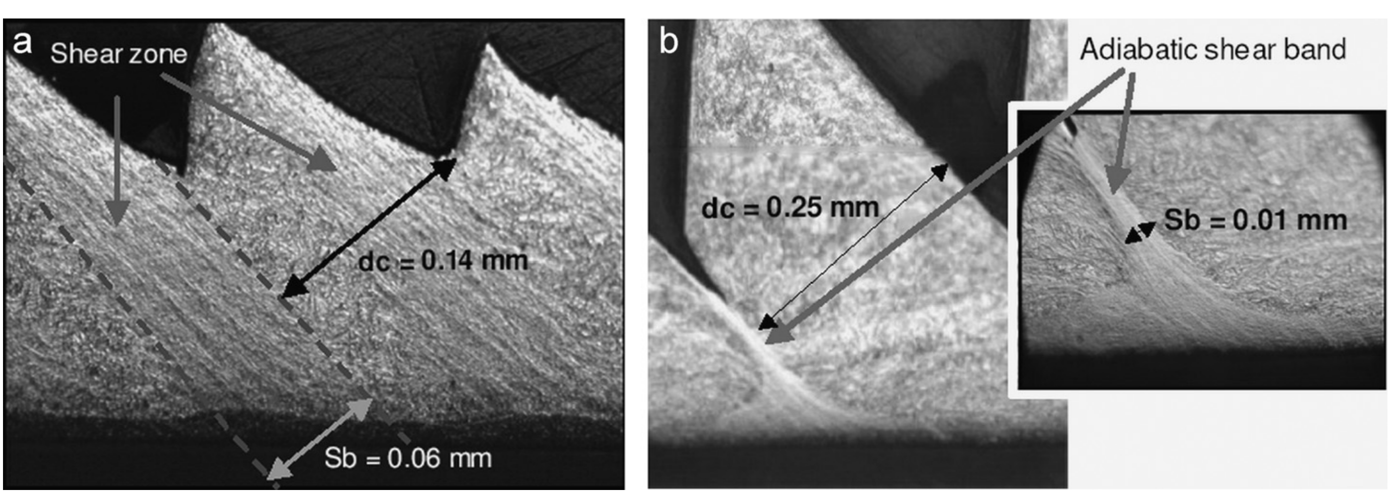

Fig. 9. Experimental: (a) Case 1 and (b) Case 2 [18].

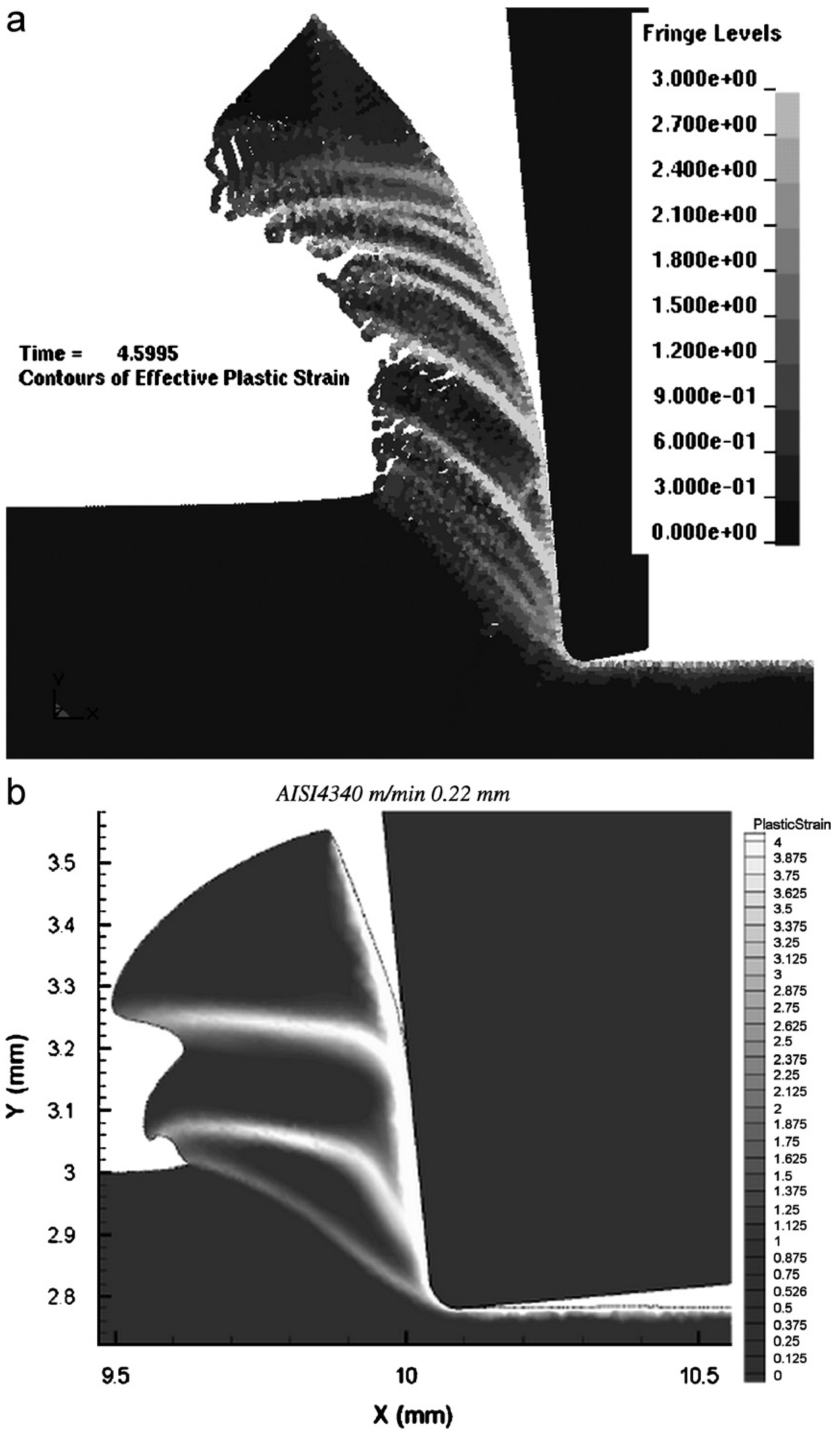

Fig. 11. Chip morphology comparisons cutting Case 1: (a) Ls-Dyna (plastic strain visual max limited to 3) and (b) Avantedge [18].

- The heating causes thermal softening of the material localized in a narrow deformation zone (Fig. 12c).
- The new formed deformation zone falls behind the tool tip and the zone is carried away into the flow (Fig. 13a). This is the end of the cycle.

In order to model shear localized chip, AdvantEdge uses a fracture model which allows for arbitrary crack initiation and propagation. An original aspect of the SPH model presented is that it does not implement a fracture model. Indeed, the fracture due to the shear localization is carried out naturally by the SPH method.

5.2.2. *Cutting forces*

Normal and tangential components of the cutting forces are compared. All simulations were performed with a 25 μm edge radius in order to minimize the introduction of

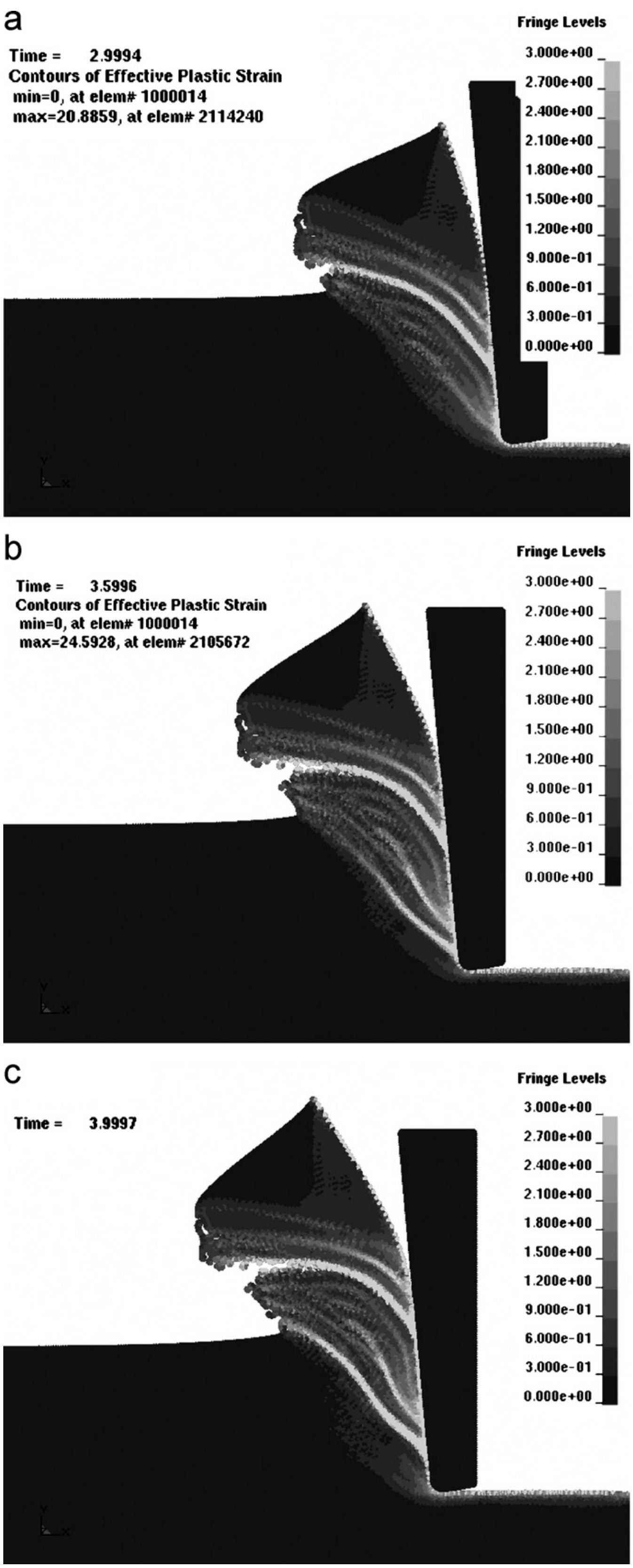

Fig. 12. Shearl localized chip formation steps cutting Case 2 Ls-Dyna ((a)–(c)) (plastic strain visual max limited to 3).

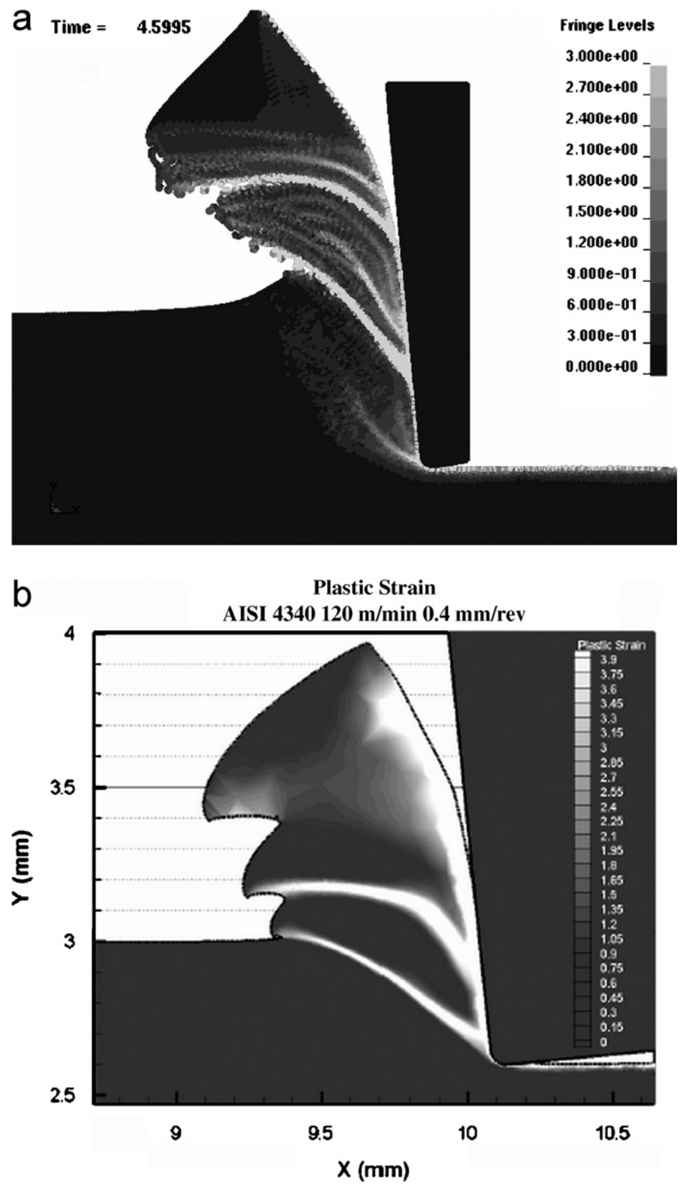

Fig. 13. Chip morphology comparisons Cutting Case 2 (a) Ls-Dyna and (b) AdvantEdge (plastic strain) [18].

an additional length scale. The Ls-Dyna and AdvantEdge cutting forces are compared in Fig. 14. Ls-Dyna predicted cutting forces agree within 15% and 35% of the measured values for, respectively, tangential and normal components. The AdvantEdge model used a Coulomb parameter fixed to 0.25 without any precision on the method to obtain this value.

6. Conclusions

The results of the implemented Ls-Dyna SPH model were compared with experimental and numerical data. The defined validation criteria were the chip morphology and the cutting forces. This study shows the relevance of the selected numerical tool. The SPH model is able to predict continuous and shear localized chips and

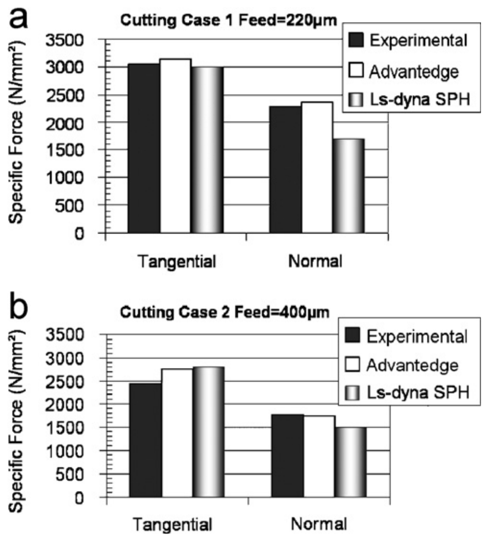

Fig. 14. AISI4340 Predicted cutting forces comparisons AdvantEdge/Ls-Dyna: (a) Case 1 and (b) Case 2.

all the steps of its formation. The model also correctly estimates the cutting forces (approximately 10% and 30% errors on, respectively, tangential and normal components) without introducing an adjusting parameter like Coulomb friction. Thus, comparable results to machining dedicated codes are obtained. The SPH model advantages are the total transparency of the assumptions made and the use of no adjusted numerical parameter (friction coefficient, fracture control parameter). Another important aspect is the meshless nature of the SPH. Indeed, no remeshing is needed to deal with high transformations problems and a ‘‘natural’’ workpiece/chip separation is thus possible.

Future work will concentrate on 3D SPH model implementation in order to deal with oblique cutting problems and more specific research on the free faces, friction and heat exchange in SPH method.

Acknowledgment

This study was carried out as part of a common research program in partnership with AIRBUS France.

References

[1] Lacome JL. Smoothed particle hydrodynamics part 1 and part 2. Contribution to LS-DYNA theory manual, Livermore Software Technology Corporation, Livermore, March 2006. ISBN: 0-9778540-0-0.

[2] Lacome JL. Analyse de la méthode particulaire SPH—Application à la détonique. PhD report, Doctorat de l'INSA, Département GMM-UMR MIP UPS, Toulouse, 1998.

[3] Marusich TD, Ortiz M. Modeling and simulation of high-speed machining. International Journal of Numerical Methods in Engineering 1995;38:3675–94.

[4] Ernst H, Merchant ME. Chip formation, friction and high quality machined surfaces. Transactions of the American Society for Metals 1941;29:299–378.

[5] Oxley PLB. The mechanics of machining. Chichester: Ellis Horwood; 1989.

[6] Moufki A, Dudzinski D, Molinari A, Rausch MA. Thermoviscoplastic modelling of oblique cutting. International Journal of Mechanical Sciences 2000;42:1205–32.

[7] Johnson GR, Cook WH. A constitutive model and data for metals subjected to large strains, high strain rates and high temperatures. In: Proceedings of the seventh international symposium on ballistics, 1983. p. 541–7.

[8] Shatla M, Kerk C, Altan T. Process modeling in machining—Part I—determination of flow stress data. Journal of Machine Tools & Manufacture 2001;41:1511–34.

[9] Özel T, Zeren E. Determination of work material flow stress and friction properties for FEA of machining using orthogonal cutting tests. Journal of Materials Processing Technology 2004;153C–154C:1019–25.

[10] Özel T. Influence of friction models on finite element simulations of machining. International Journal of Machine Tools and Manufacture 2006;46:518–30.

[11] Bil H, Engin S, Erman Tekkaya A. A comparison of orthogonal cutting data from experiments with three different finite element models. International Journal of Machine Tools and Manufacture 2004;44(9):933–44.

[12] Guétaria Y, Le Corre S, Moës N. Etude des possibilités de la méthode X-FEM pour la simulation numérique de la coupe. Mécanique & Industries 2005;6:315–9.

[13] Oliver J, Cante JC, Gonzalez C. On particle finite element methods in solid mechanics problems. Computational Plasticity/COMPLAS VIII, vol. 1, 2005. p. 82–5.

[14] Irander CG. Verifiering av simuleringsdata. PhD thesis, Lahue Tekniska Universitet, 2004.

[15] Batra RC, Zhang GM. Analysis of adiabatic shear bands in elasto-thermo-viscoplastic materials by modified smoothed-particle hydrodynamics (MSPH) method. Journal of Computational Physics 2004;201:172–90.

[16] Lesuer DR, Leblanc MM, Kay GJ. Modeling large-strain high rate deformation metals. Technical report UCRL-JC-134118, Lawrence Livermore National Laboratory, 2001.

[17] Marusich TD. Effects of friction and cutting speed on cutting force. ASME, MED-23313, 2001. p. 115–23.

[18] Mabrouki T, Deshayes L, Ivester R, Rigal JF, Jurrens K. Material modelling and experimental study of serrated chip morphology. 7th CIRP, 2004.

[19] Davies MA, Burns TJ. Thermomechanical oscillations in material flow during high-speed machining. Philosophical Transactions of the Royal Society of London 2001;359:821–46.

[20] Anon., LS-DYNA Keyword User's Manual Version 970, Livermore Software Technology Company, Livermore, March 2006. ISBN: 0-9778540-2-7.